

# A Lightweight Robotic Arm with Pneumatic Muscles for Robot Learning

Dieter Büchler, Heiko Ott, Jan Peters

{dieter.buechler, heiko.ott, jan.peters} @ tue.mpg.de

**Abstract**—Versatile motor skills for hitting and throwing motions can be observed in humans already in early ages. Future robots require high power-to-weight ratios as well as inherent long operational lifetimes without breakage in order to achieve similar perfection. Robustness due to passive compliance and high-speed catapult-like motions as possible with fast energy release are further beneficial characteristics. Such properties can be realized with antagonistic muscle-based designs. Additionally, control algorithms need to exploit the full potential of the robot. Learning control is a promising direction due to its the potential to capture uncertainty and control of complex systems.

The aim of this paper is to build a robotic arm that is capable of generating high accelerations and sophisticated trajectories as well as enable exploration at such speeds for robot learning approaches. Hence, we have designed a light-weight robot arm with moving masses below 700 g with powerful antagonistic compliant actuation with pneumatic artificial muscles. Rather than recreating human anatomy, our system is designed to be easy to control in order to facilitate future learning of fast trajectory tracking control. The resulting robot is precise at low speeds using a simple PID controller while reaching high velocities of up to 12 m/s in task space and 1500 deg/s in joint space. This arm will enable new applications in fast changing and uncertain task like robot table tennis while being a sophisticated and reproducible test-bed for robot skill learning methods. Construction details are available.

## I. INTRODUCTION

An intended outcome of robotics research is to make robots help humanity by taking over simple work. This is already achieved for industrial applications like pick-and-place tasks where robots move along a predefined and henceforth unchanged trajectory. However, when it comes to uncertain, high-dimensional and fast-changing tasks, e.g. walking and running for humanoid robots (see Darpa Robotics Challenge 2015 [8]) or playing table tennis with an anthropomorphic arm [18], robots are not able to reach the performance of humans. The explanation lies in the interplay between control algorithms that cannot fully use the potential of the given system and the robot hardware design that makes control of versatile movements problematic. The human arm design owns many beneficial properties that widen the range of possible trajectories, thus enrich the variety of tasks being able to fulfill. For instance, it enables to lift heavy objects and generate high accelerations at the end-effector. Hence high velocities can be reached over a small distance which enables

This work was supported by the Max Planck Institute for Intelligent Systems.

All authors are affiliated with the MPI for Intelligent Systems, Spe-mannstr. 38, 72076 Tübingen, Germany. Dieter Büchler and Jan Peters are also with TU Darmstadt, Hochschulstr. 10, 64289 Darmstadt, Germany

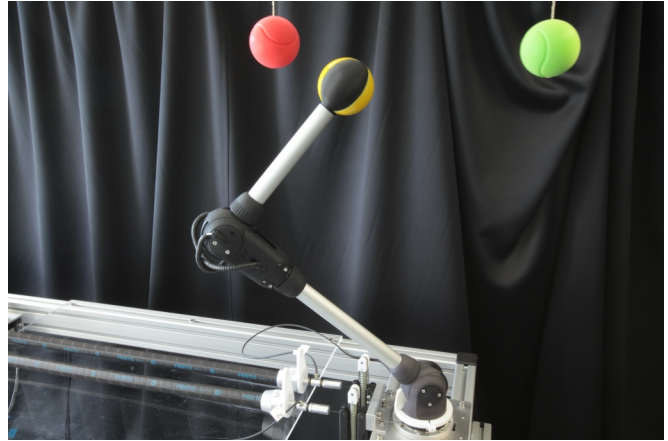


Fig. 1. Igus robolink lightweight arm (700 g) with a rotational and swivel degree of freedom within each joint. It is actuated by 8 pneumatic artificial muscles.

fast reaction times. Concurrently, the human arm is robust due to the soft skin, inhibiting damage at collisions and the built-in passive compliance which ensures the deflection of the end-effector instead of breakage as a response to external forces. Robustness against errors in control is an additional benefit of compliance e.g. for grasping, moving objects (fitting objects into a tight form) or for fast changing tasks where full precision cannot be achieved like in table tennis.

Robotic arms actuated by antagonistic pneumatic artificial muscle (PAM) pairs incur some of these abilities. In addition, such systems are interesting from a control point of view as they pose hard challenges like non-linearities, time-varying behavior (as a result of dependencies on temperature and wearing) as well as hysteresis effects [4], [28]. Also, PAMs show similarities to skeletal muscles in static and dynamic behavior [6], [16], [25], [7]. Learning precise, fast and adaptable control of such actuation mechanisms may establish the base for advances in building more complicated robots with preferable abilities.

However, PAMs do not resemble the skeletal muscle to the full extent. PAMs pull only along their linear axes and break as well as wear out when curled. Muscle structures bending over bones like the deltoid muscles that connects the acromion with the humerus bone at the shoulder are hardly realizable. Furthermore, biological muscles can be classified as wet-ware whereas PAMs suffer from additional friction when touching each other or the skeleton during usage. Thus,

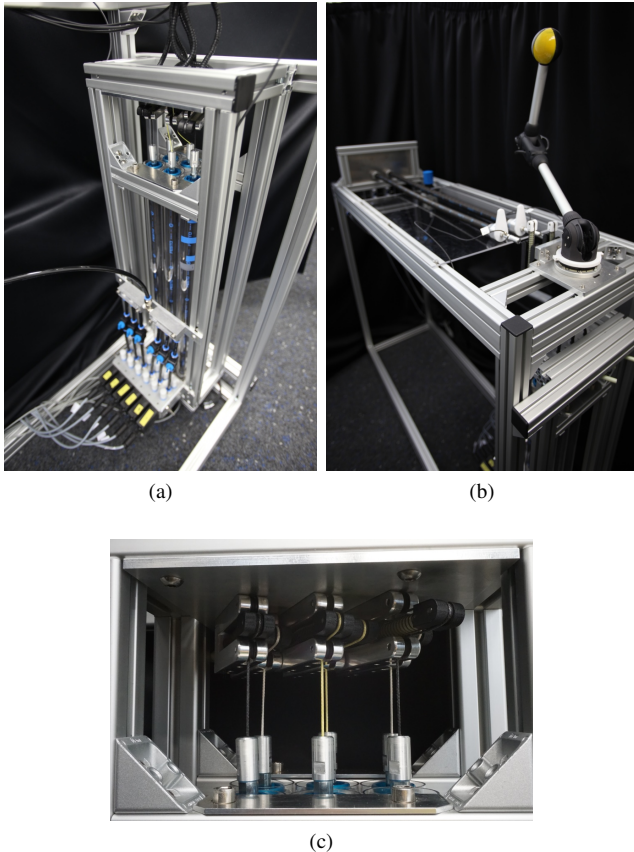


Fig. 2. Hardware components designed to keep friction low. (a) 6 PAMs are located directly below the Igus arm in order to pull the cables in the same direction as they exit the arm so that deflection is minimized. Necessary bending of the cables is realized by Bowden cables. (b) 2 PAMs actuating the first DoF are located on top of the base frame. They are longer than the other 6 PAMs due to the bigger radius of the first rotational movement. (c) Cables need pretension to not slip off the guidances within the arm. Springs push a roll to wind up the remaining cable length. This happens mainly if the robot is not pressurized.

bi-articular configurations (influencing 2 DoFs) like present in the human arm with 7 DoFs are hard to realize. Moreover, non-linear effects in actuation become more severe in case high weights have to be accelerated. Although it seems that PAMs are well suited to be attached directly to the joints instead of using cables due to their high power-to-weight ratio, a stable and hence heavy skeleton is necessary.

Still, many systems have been designed that aim at reproducing human anatomy by using pneumatic artificial muscles. For our purpose it is crucial that anthropomorphism does not hinder the controllability of the resulting arm. Although recent publications show good tracking performance of one PAM in position [31], [29], [2], using PAM-based systems with more DoFs for fast trajectory tracking appears to be less satisfactory although control algorithms could be successful on a system that is engineered to support fast motions. The performance of PAM-actuated robots has thus been limited to slow movements compared to servo motor driven robots. In table I, existing PAM-actuated arms are listed along with the most complex (form and velocity)

tracked trajectory in case it was mentioned. We identify the following key problems for building a robotic arm for our intended task: 1) friction between muscles, 2) friction between muscles and skeleton, 3) high-dimensionality without modularity, 4) increased moving mass due to PAMs attached to joints directly, 5) additional static friction due to deflection of cables, 6) heavy-weight segments, 7) largely dependent DoFs.

Learning control algorithms have been incorporated for fast-changing and uncertain task like table tennis [17]. Desired extensions for the robotic systems were, on the one hand, the ability to generate higher accelerations to reach similar velocities over shorter distances and, on the other hand, robustness for exploration at high velocities. The latter is essential for learning striking motions. As a result, successful approaches in simulations usually have to be constrained for safety purposes on the real robot.

For the before-mentioned reason, we aim at creating a robot that fulfills our requirements while avoiding the problems above in order to achieve precise and *fast* movements. Therefore, we use the lightweight and tendon-driven Igus Robolink arm (see Fig. 1) with four degrees of freedom (DoF) actuated by eight PAMs. We want to highlight that we do not intend to build a safe robot in terms of collaborating with humans or other robots as the release of stored energy in the antagonistic PAM pair can always lead to collisions with nearby object. Our robot is designed in a way that it can physically sustain high velocities at the end-effector and ensure to stay within predefined joint ranges due to the antagonistic configuration of two PAMs. Motions generated by one PAM can be countered with the antagonistic PAM by applying a minimum pressure and decelerate before damage can happen. We show the effectiveness of this design in section III.

We encourage other researcher to use our platform as a testbed for learning control approaches. We used off-the-shelf and affordable parts like PAMs by Festo, the robotic Arm by Igus and build the base using Item profiles. All necessary documents to rebuild our system as well as a video of its performance can be found at <http://ei.is.tuebingen.mpg.de/person/dbuechler>.

The paper is structured as follows: A technical description of the arm is given in section II. Experiments in section III show high velocity and acceleration profiles highlighting the robustness of the system. A simple manually tuned PID controller is utilized to follow slow trajectories for all four DoF simultaneously emphasizing the largely independent DoFs due to low moving masses as well as beneficial construction considerations. We briefly summarize and discuss the implications of the setup in section IV.

## II. HARDWARE CONFIGURATION

This arm has been built to facilitate precise and fast control. We do so by using a light-weight 2-link tendon-driven arm by Igus [14] with a swivel and rotational DoF in each of the two joints. Each DoF is actuated by two antagonistically aligned Festo fluidic muscles pairs. The contraction ratio as

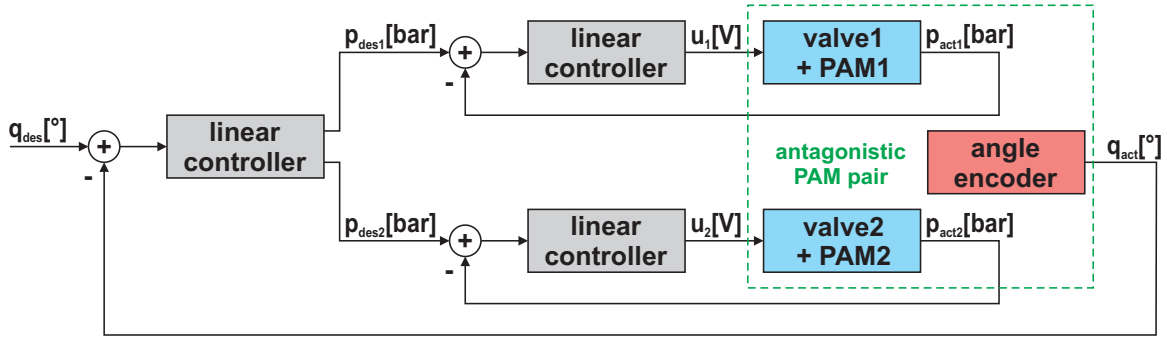


Fig. 3. Schematic description of the position control loop for one PAM muscle pair. The absolute value of the output signal of the position control PID receives one of both muscle dependent on the sign of this signal. The other PAM is set to its individual minimum pressure. The pressure within each PAM is governed by separate PIDs that set the input voltage to the proportional air flow valves. The sensor values are provided by Festo pressure sensors and angle encoders.

well as the pulling force is influenced by the air pressure within each PAM. Thus, a linear controller regulates the pressure within each PAM using Festo proportional valves. As a result, the control algorithm that regulates the movement works on top of these. In the following, we present the characteristics of the elements utilized for the arm along with the connection to our guidelines.

#### A. Igus Robolink light-weight arm

The Igus Robolink arm is especially suitable for minimizing non-linearities and dependencies between DoFs due to high moving masses. Two links and the elbow joint weigh together less than 700 g. The first joint which is fixed to the base contributes minor to the moving mass. In addition, it is driven by Dyneema tendons (2mm diameter, tensile strength of 4000 N) that allow to fix the PAMs in the base. Necessary deflections within the Igus arm are realized through Bowden cables. They guide the cables within the arm and keep the length unchanged during movement. This enables to actuate each DoF mostly independently. Still little cross-talking between the DoFs persists as the PAMs share the same air pressure supply as well as due to the non-zero moving mass. The arm can be easily extend to a higher

number of DoF because of its modular structure.

Cable-driven systems usually suffer from additional friction. For this reason, the tendons are only minimally bended by our construction. All PAMs pull their respective tendons in the same direction as they exit the Igus arm. Two PAMs actuate the first rotational DoF in the base joint in horizontal orientation whereas the other 6 PAMs pull in vertical direction as can be seen in Fig. 2 (a) and (b), respectively. Fig. 2 (c) displays the pretension mechanism that prevents the cables from jumping out of the guidances within the arm. The joint angles are measured by angular encoders with a resolution of approximately  $0.07^\circ$ . The kinematic structure is depicted in Fig. 4(b).

#### B. Pneumatic Artificial Muscles

We use pneumatic artificial muscles by Festo to actuate the robotic arm. Off-the-shelf PAMs were incorporated as we want to facilitate the rebuilding process. They consist of an inner rubber tube surrounded by a braided weave composed of repeated and identical rhombuses. An increase in air pressure leads to a gain in diameter of the inner balloon. The double-helix-braided sheave transforms the axial elongation into a longitudinal contraction. This complete process can be

TABLE I

A COLLECTION OF PNEUMATIC BASED ROBOTIC ARM-LIKE SYSTEMS IS LISTED NEXT TO THE NUMBER OF DOFS IN JOINT SPACE AND THE FASTEST AND MOST COMPLEX TRACKED TRAJECTORY IN CASE IT HAS BEEN MENTIONED.

YEAR	PUBLICATION	# DoF	FASTEST AND MOST COMPLEX TRAJECTORY TRACKED
2014	Rezoug et al. [22]	7	Sinusoidal reference with $f=1$ Hz for one DoF
2012	Hartmann et al. [12]	7	Sinusoidal reference in task space ( $x: 1$ Hz, $y: 2$ Hz, $z$ not tracked)
2012	Ikemoto et al. [15]	7 (17 PAMs)	Human taught reference (similar to sinusoidal) periodic with $f=\text{appr.}0.33$ Hz
2009	Ahn and Ahn [1]	2	triangular reference with 0.05 Hz
2009	Shin et al. [23]	1 (4 PAMs)	Sinusoidal reference with $f=6$ Hz for one DoF
2009	Van Damme et al. [30]	2 (4 PAMs)	Sinusoidal reference with $f=0.33$ Hz for both DoF
2007	Festo Airic's arm [10]	7 (30 PAMs)	-
2006	Thanh and Ahn [24]	2	Circle with 0.2 Hz using both DoFs
2005	Hildebrandt et al. [13]	2	Step and sinusoidal reference with 0.5 Hz
2005	Tondu et al. [26]	7	-
2004	Boblan et al. [3]	7 in arm	-
2000	Tondu and Lopez [27]	2	independent sinusoidal activation of each DoF with 0.1 Hz
1998	Caldwell et al. [5]	7	Response of shoulder joint to $90^\circ$ step reference
1995	Caldwell et al. [4]	7	Response to a square wave reference input (0.2 Hz, 1 DoF)

fully characterized according to the radius of the inner tube and the braid angle. The inner pressure plays the same role as the neuronal activation level of a biological muscle. The dynamics of both, PAMs and biological muscles, are known to follow the Hill muscle model [6], [16], [25]

$$(F + a)(V + b) = b(F_0 + a), \quad (1)$$

where  $F$  and  $V$  are the tension and contraction velocity of the muscle,  $a$  and  $b$  muscle-dependent empirical constants and  $F_0$  the maximum isometric force generated in the muscle. Also the static behavior of PAMs is in accordance to biological muscles [7].

PAMs have been mainly applied due to their safety properties and high power-to-weight ratio for slow movements with the ability to carry heavy objects. Challenging in term of control is the non-linear relationship between length, contraction velocity and pressure as well as problematic effects like temperature dependency, time-variance and hysteresis [28].

Despite these issues, PAMs have beneficial properties we try to exploit here. We use two 1 m and six 0.6 m long PAMs with a diameter of 20 mm which can generate maximum forces of up to 1500 N at 6 bar. We limit the pressure to a maximum of 3 bar because the generated accelerations are sufficient and due to safety precautions. Powerful actuation can easily overcome the resisting force of static friction and the antagonistic muscle pair configuration reduces the overshoot in velocity. Also, fast and catapult-like movements can be generated by pressurizing both PAMs and discharging one of them. This kind of energy storage and release can also be found in human and primate arms. Especially for tasks like table tennis this property can be valuable.

At such high velocities, antagonistic muscle structures can additionally be used to avoid damaging the robot. Our system is designed in such a way that the arm never exceeds fixed joint limits by supplying an individual minimum pressure to counter the movement generated by the respective antagonistic PAM. Thus, the oppositely acting PAMs avoid damages occurring due to undesired motions. Robotic systems with servomotors must take care not to reach too high accelerations as the movement might not be decelerated fast enough. Moreover, PAMs are open loop position stable, meaning that the set signal does not have to be zero in order to reach equilibrium. By contrast, servo motors open loop velocity stable [28].

Another useful property is the inherent compliance that adds robustness to task fulfillment if the trajectory cannot be tracked perfectly. For instance, touching an object with an compliant actuator is easier as the velocity must not be absolute zero in order to not damage the robot or the object. Using active compliance on a servo-motor based robotic system requires high sampling rates in order to react external forces in real-time.

### C. Software Framework

The complete system comprises eight pressure sensors and proportional valves as well as four incremental angular encoders to govern and describe the movement. Control is

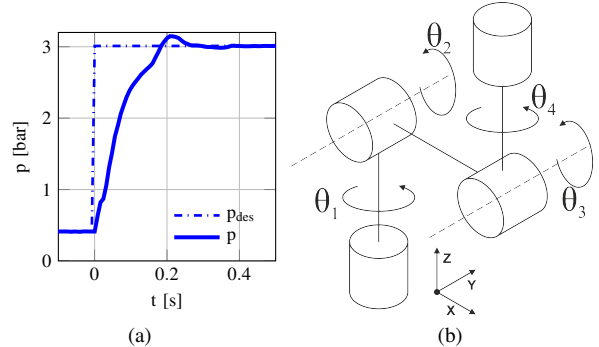


Fig. 4. (a) Pressure step response from minimum to maximum value of 3 bar. The desired pressure value can be reached within approximately 250 ms. (b) Kinematic structure of the Iguis Robolink arm. A rotational DoF is located at the base ( $\theta_1$ ) and the end-effector ( $\theta_4$ ). Two swivel DoFs ( $\theta_2$  and  $\theta_3$ ) are placed in between.  $\theta_1$  and  $\theta_2$  are realized in joint 1 and  $\theta_3$  and  $\theta_4$  in joint 2.

eased by delegating low level task, such as extraction of the angular value from the A and B digital signals given by the encoder or regulating the pressure within each PAM. The National Instruments PCIe 7842R FPGA card has been used to take over these tasks and govern the communication with the hardware. The FPGA was programmed in Labview. To assure fast implementation, we used the FPGA Interface C API to generate a bitfile along with header files which can be incorporated in any C project. Thus, the control algorithm can be implemented in C on top of the basic functionalities supplied by the FPGA. The sensor values are read with 10 kHz and new desired pressure values are adjusted at 1 kHz. Fig. 4(a) shows the pressure response to a step in desired value from minimum (0 bar) to maximum air pressure (3 bar). The resulting pressure regulation reaches the desired value within a maximum of 0.25 seconds.

## III. EXPERIMENTS

Our robotic arm has a modular structure that allows to control each DoF almost independently. We show that by tracking ramp-like signals as well as a sinusoidal reference in joint space for each DoF separately. In addition, high velocity and acceleration profiles are demonstrated to underline the ability of the arm to be utilized for hitting and catapult-like motions while avoiding damages at such paces.

### A. PID Control

We use a simple PID controller to track predefined trajectories in joint-space. The underlying control law

$$u = K_p \tilde{q} + K_d \dot{\tilde{q}} + K_i \int_0^t \tilde{q}(x) dx, \quad (2)$$

with the position and velocity error  $\tilde{q} = q_{des} - q$  and  $\dot{\tilde{q}}$ , can be adjusted to a system by changing the position, velocity and integral gains  $K_p$ ,  $K_d$  and  $K_i$ . We tuned both the pressure and the position regulating PIDs manually.

PIDs are widely used in industry because of their simple implementation and intuitive tuning procedure. However, they are not well suitable for tracking tasks. Besides that, a

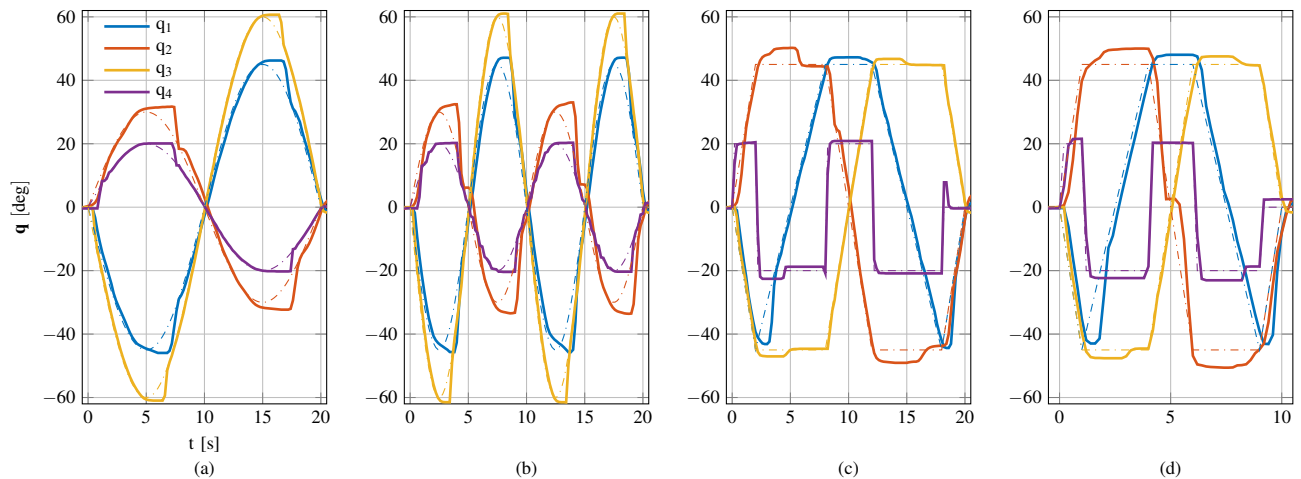


Fig. 5. The tracking performance shows satisfactory results using a manually-tuned PID controller. Some overshoots for rapid change in reference signals are visible that cannot be compensated. For smooth changes in (b) the trajectory is tracked sufficiently good. (a) Sinusoidal reference with  $f=0.05$  Hz. (b) Sinusoidal reference with  $f=0.1$  Hz. (c) Truncated ramp reference for DoF 1 to 3 and rectangular reference for DoF 4. (d) Same reference as in (a) but twice as fast.

strong coupling between the DoFs confines its application. In addition, the position feedback is always delayed by at least one cycle and the integral sum takes some iterations for correction in case the reference suddenly changes. Nevertheless, integration of position errors is necessary if gravitation is present. For position regulation, the controller output  $u$  must set the desired pressure for both PAMs  $p_{des,1}$  and  $p_{des,2}$  of an antagonistic pair. We discriminate by considering the sign of the control signal. Depending on the sign one of both PAMs is set to the absolute value of the control signal  $u$  while the other is assigned with an individual minimum pressure  $p_{min,1}$  or  $p_{min,2}$  respectively

$$p_{des,1} = \begin{cases} |u| \\ p_{min,1} \end{cases} \quad p_{des,2} = \begin{cases} p_{min,2} & \text{if } u \geq 0 \\ |u| & \text{otherwise.} \end{cases} \quad (3)$$

The schematic description of pressure and position regulation representative for each antagonistic muscle pair is depicted in Fig. 3.

### B. PID Tracking

The aim is to highlight the modularity and low controlling demands of the arm by showing that adequate tracking performance is possible using linear controllers only. Therefore, we track all 4 DoFs simultaneously for two kinds of reference signals as can be seen in Fig. 5. In (a) and (c) a truncated triangular signal was tracked in 10 and 20 seconds, respectively. All graphs show that for rapidly changed references, tracking becomes inaccurate. This is mainly due to the general problems with PID controllers mentioned above but also due to the distribution of the controller output signal. For fast correction, the PAM countering the movement has to start pulling beginning at its maximum elongation as the minimum pressure has been set. Thus, in the first moments the contraction of the PAM has no effect on the joint angle. For severe cases, this forbearance is followed by a too strong correction as can be seen for DoF 2 in Fig. 5 (a) and (c) for

the middle part of the graph. This DoF drives the most mass and hence is harder to control precisely compared to the other DoFs. A controller that allows co-contraction of both PAMs may solve this problem.

Sub-figures (b) and (d) show tracked sinusoidal references with 0.05 and 0.1 Hz. Here the same issues occur for rapid changes of the reference. However, for smooth changes the reference can be followed with some small delay with all DoF. This emphasizes that the stiction level in the system is low.

### C. Maximum Velocity and Acceleration Profiles

High accelerations are necessary to reach high velocities on a short distance to enable a versatile bouquet of possible trajectories and fast reaction. Our system can generate high velocities and accelerations due to the strength of the PAMs used while being robust as a result of the antagonistic muscle configuration. This is critical for exploration of fast hitting motions using learning control methods.

To show this, a fast trajectory was generated using the swivel DoF 2 and 3. The respective minimum pressure was set to one of the PAMs of each muscle pair while the maximum pressure was assigned to the corresponding PAM. The subsequent switching from maximum to minimum in each PAM generated a fast trajectory at the end-effector as can be seen in Fig. 6 (a). Note that this set signal generates the fastest movement at the end-effector that a closed loop controller could have determined. We did not find any other set signal that moved the arm that near to its joint limits and generated such high peak velocities and accelerations. For this reason, we renounced on performing this experiment in closed loop. The task space  $\mathbf{x} = [x_1, x_2, x_3]^T$  has been determined from the joint space coordinates  $\mathbf{q} = [q_1, q_2, q_3, q_4]^T$  for each data-point using the forward kinematics equations  $\mathbf{x} = T_x^q(\mathbf{q})$ . Fig. 4 (b) makes the derivation of the forward kinematics equations easy. We do not consider the orientation of the end-effector here. The resulting velocity and

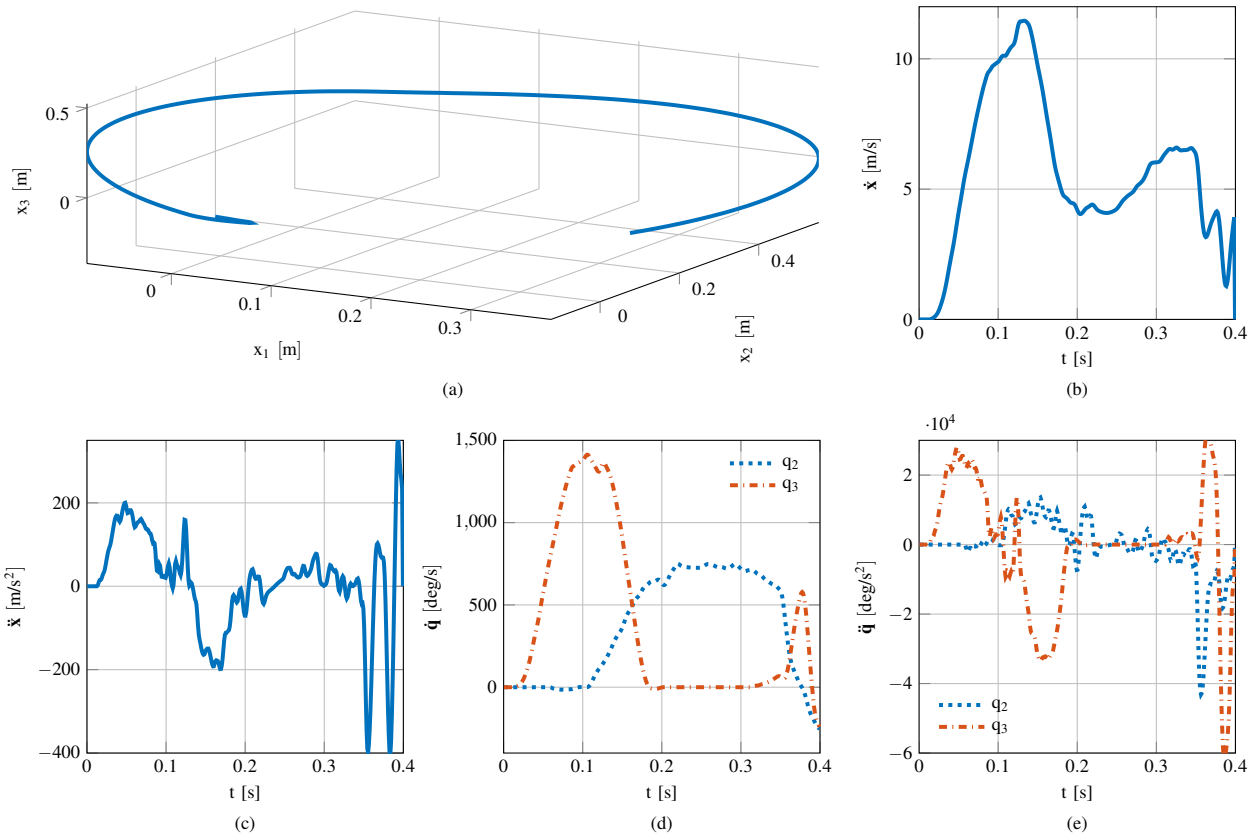


Fig. 6. High velocity and acceleration profiles in task and joint space. DoF 2 and 3 were actuated with the maximum pressure moving in between the joint limits. (a) Trajectory of the end-effector in task space. (b) Velocity profile along the trajectory in (a). Maximum value is 12m/s. (c) Acceleration profile along the trajectory in (a). The maximum value reaches up to 200  $m/s^2$ . (d) Angular velocity profile for both swivel DoF. DoF 3 is faster as it has to accelerate less weight than DoF 2. The maximum value of about 1500  $deg/s$  is reached with DoF 3. (e) Angular accelerations show a maximum of approximately 28000  $deg/s^2$

acceleration profiles, depicted in (b) and (c), show at their respective maxima approximately 12  $m/s$  and 200  $m/s^2$ . As a comparison, the fast Barrett Wam arm that has been used for table tennis [18], can generate peak velocities of 3  $m/s$  and peak accelerations of 20  $m/s^2$ . The resulting angular velocities in DoF 3 reaches up to 1500  $deg/s$  and angular acceleration of 28000  $deg/s^2$ .

#### IV. CONCLUSION

A lightweight robotic arm with four DoFs actuated by eight pneumatic artificial muscles has been designed using only off-the-shelf components. We considered other PAM-actuated robotic arms to adapt the construction for our purpose.

##### A. Discussion and Summary of Contributions

Although we could easily extend the Igus robotic arm to more DoFs, we renounced on constructing a too complex system to avoid running into many problems at once. Still skillful motion are possible with four DoFs as only three DoFs are needed to reach each point in the workspace. Having this system, the success in task fulfillment depends on the control algorithm. Although this robot has the capability to perform well in hitting and striking tasks, demands are high

for the controlling part as such tasks require fast decision making and precise control.

To our knowledge, no muscle based system has been designed to reach the same velocities and accelerations in task space as our robotic arm while being sufficiently robust. We achieved that by minimizing the weight that needs to be moved and used powerful PAMs. The antagonistic muscle configuration assured that joint limits are not reached despite of the high kinetic energy. Control has been eased due to the avoidance of bending of the tendons as well as the antagonistic muscle pair configuration. Sufficient tracking performance has been shown incorporating simple and manually tuned linear controllers.

##### B. Future Work

Taking humans as an example of successful systems that are able to overcome the non-linearities, task uncertainty and high-dimensionality of the human motor system, learning control is a promising direction. Experiments provide compelling evidence for the employment of Reinforcement Learning (RL) in the human sensorimotor learning system [20]. In particular, model-based RL which is known for its high sample efficiency [9] relies on precise internal models. Involvement of forward models in human motor learning can be verified on the behavioral level [11].

Recent advances in Machine Learning show that human like performance can be achieved. For instance, combinations of Neural Networks with Reinforcement Learning [19] proved to extract knowledge from high-dimensional data and use it to play Atari games, mostly better than human professionals do. Another promising direction are probabilistic kernel methods like Gaussian Processes [21]. They can be incorporated to learn from previous experience and give notion of how certain the computed solution is given the data.

In our future work, we want to implement sophisticated learning control approaches that are a combination of the different directions mentioned above. After achieving better performance we will extend the arm to more DoFs and want to test whether bi- and tri-articular configurations can be beneficial for our class of tasks.

In order to accelerate the advances in the this field, we encourage other researcher to rebuild our system and test learning control approaches. Construction details are available online (<http://ei.is.tuebingen.mpg.de/person/dbuechler>). We tried to make a step towards enabling plug-and-play of successful learning control approaches in simulation to a real system. Also improvements of our design will be updated and it is desired to share further advances in an open source manner.

#### REFERENCES

- [1] Kyoung Kwan Ahn and Ho Pham Huy Anh. Design and implementation of an adaptive recurrent neural networks (ARNN) controller of the pneumatic artificial muscle (PAM) manipulator. *Mechatronics*, 19(6):816–828, September 2009.
- [2] G. Andrikopoulos, G. Nikolakopoulos, I Arvanitakis, and S. Manesis. Piecewise Affine Modeling and Constrained Optimal Control for a Pneumatic Artificial Muscle. *IEEE Transactions on Industrial Electronics*, 61(2):904–916, February 2014.
- [3] Ivo Boblan, Rudolf Bannasch, Hartmut Schwenk, Frank Prietzel, Lars Miertsch, and Andreas Schulz. A Human-Like Robot Hand and Arm with Fluidic Muscles: Biologically Inspired Construction and Functionality. In Fumiya Iida, Rolf Pfeifer, Luc Steels, and Yasuo Kuniyoshi, editors, *Embodied Artificial Intelligence*, number 3139 in Lecture Notes in Computer Science, pages 160–179. Springer Berlin Heidelberg, January 2004.
- [4] Darwin G. Caldwell, Gustavo A. Medrano-Cerda, and Mike Goodwin. Control of pneumatic muscle actuators. *Control Systems, IEEE*, 15(1):40–48, 1995.
- [5] D.G. Caldwell, N. Tsagarakis, D. Badihi, and G.A. Medrano-Cerda. Pneumatic muscle actuator technology: a light weight power system for a humanoid robot. In *1998 IEEE International Conference on Robotics and Automation, 1998. Proceedings*, volume 4, pages 3053–3058 vol.4, 1998.
- [6] Ching-Ping Chou and B. Hannaford. Measurement and modeling of McKibben pneumatic artificial muscles. *IEEE Transactions on Robotics and Automation*, 12(1):90–102, 1996.
- [7] Ching-Ping Chou and Blake Hannaford. Static and dynamic characteristics of McKibben pneumatic artificial muscles. In *Robotics and Automation, 1994. Proceedings., 1994 IEEE International Conference on*, pages 281–286. IEEE, 1994.
- [8] Darpa. Darpa Robotics Challenge, 2015.
- [9] Marc Peter Deisenroth, Gerhard Neumann, and Jan Peters. A Survey on Policy Search for Robotics. 2013.
- [10] Festo. Airics arm. 2007.
- [11] Adrian M. Haith and John W. Krakauer. Model-Based and Model-Free Mechanisms of Human Motor Learning. In Michael J. Richardson, Michael A. Riley, and Kevin Shockley, editors, *Progress in Motor Control*, number 782 in Advances in Experimental Medicine and Biology, pages 1–21. Springer New York, January 2013.
- [12] Christoph Hartmann, Joschka Boedecker, Oliver Obst, Shuhei Ikemoto, and Minoru Asada. Real-Time Inverse Dynamics Learning for Musculoskeletal Robots based on Echo State Gaussian Process Regression. In *Robotics: Science and Systems*, 2012.
- [13] A. Hildebrandt, O. Sawodny, R. Neumann, and A. Hartmann. Cascaded control concept of a robot with two degrees of freedom driven by four artificial pneumatic muscle actuators. In *American Control Conference, 2005. Proceedings of the 2005*, pages 680–685 vol. 1, 2005.
- [14] Igus. Robolink light-weight robotic arm. 2015.
- [15] S. Ikemoto, Y. Nishigori, and K. Hosoda. Direct teaching method for musculoskeletal robots driven by pneumatic artificial muscles. In *2012 IEEE International Conference on Robotics and Automation (ICRA)*, pages 3185–3191, May 2012.
- [16] G.K. Klute, J.M. Czerniecki, and B. Hannaford. McKibben artificial muscles: pneumatic actuators with biomechanical intelligence. In *1999 IEEE/ASME International Conference on Advanced Intelligent Mechatronics, 1999. Proceedings*, pages 221–226, 1999.
- [17] Katharina Mlling, Jens Kober, Oliver Kroemer, and Jan Peters. Learning to select and generalize striking movements in robot table tennis. *The International Journal of Robotics Research*, 32(3):263–279, March 2013.
- [18] Katharina Mlling, Jens Kober, and Jan Peters. A biomimetic approach to robot table tennis. *Adaptive Behavior*, 19(5):359–376, October 2011.
- [19] Volodymyr Mnih, Koray Kavukcuoglu, David Silver, Andrei A. Rusu, Joel Veness, Marc G. Bellemare, Alex Graves, Martin Riedmiller, Andreas K. Fiedjeland, Georg Ostrovski, Stig Petersen, Charles Beattie, Amir Sadik, Ioannis Antonoglou, Helen King, Dharmsharan Kumaran, Daan Wierstra, Shane Legg, and Demis Hassabis. Human-level control through deep reinforcement learning. *Nature*, 518(7540):529–533, February 2015.
- [20] John P O’Doherty, Sang Wan Lee, and Daniel McNamee. The structure of reinforcement-learning mechanisms in the human brain. *Current Opinion in Behavioral Sciences*, 1:94–100, February 2015.
- [21] Carl Edward Rasmussen and Christopher K. I Williams. *Gaussian processes for machine learning*. MIT Press, Cambridge, Mass., 2006.
- [22] A. Rezoug, B. Tondu, and M. Hamerlain. Experimental Study of Nonsingular Terminal Sliding Mode Controller for Robot Arm Actuated by Pneumatic Artificial Muscles. 2014.
- [23] Dongjun Shin, Irene Sardellitti, Yong-Lae Park, Oussama Khatib, and Mark Cutkosky. Design and Control of a Bio-inspired Human-friendly Robot. *The International Journal of Robotics Research*, November 2009.
- [24] TU Diep Cong Thanh and Kyoung Kwan Ahn. Nonlinear PID control to improve the control performance of 2 axes pneumatic artificial muscle manipulator using neural network. *Mechatronics*, 16(9):577–587, November 2006.
- [25] B. Tondu and S.Zagal Diaz. McKibben artificial muscle can be in accordance with the Hill skeletal muscle model. In *The First IEEE/RAS-EMBS International Conference on Biomedical Robotics and Biomechanics, 2006. BioRob 2006*, pages 714–720, 2006.
- [26] B. Tondu, S. Ippolito, J. Guiochet, and A. Daidie. A Seven-degrees-of-freedom Robot-arm Driven by Pneumatic Artificial Muscles for Humanoid Robots. *The International Journal of Robotics Research*, 24(4):257–274, April 2005.
- [27] B. Tondu and P. Lopez. Modeling and control of McKibben artificial muscle robot actuators. *IEEE Control Systems*, 20(2):15–38, 2000.
- [28] Bertrand Tondu. Modelling of the McKibben artificial muscle: A review. *Journal of Intelligent Material Systems and Structures*, 23(3):225–253, February 2012.
- [29] Bertrand Tondu. Robust and Accurate Closed-Loop Control of McKibben Artificial Muscle Contraction with a Linear Single Integral Action. *Actuators*, 3(2):142–161, June 2014.
- [30] Michel Van Van Damme, Bram Vanderborght, Bjorn Verrelst, Ronald Van Ham, Frank Daerden, and Dirk Lefeber. Proxy-based Sliding Mode Control of a Planar Pneumatic Manipulator. *The International Journal of Robotics Research*, 28(2):266–284, February 2009.
- [31] Jun Zhong, Jizhuang Fan, Yanhe Zhu, Jie Zhao, and Wenjie Zhai. One Nonlinear PID Control to Improve the Control Performance of a Manipulator Actuated by a Pneumatic Muscle Actuator. *Advances in Mechanical Engineering*, 6:172782, May 2014.